Geophys. Astrophys. Fluid Dynamics, Vol. 87, pp. 215–252

THERMAL CONVECTION IN A ROTATING FLUID ANNULUS BLOCKED BY A RADIAL BARRIER

Q. G. RAYER [a], D. W. JOHNSON [b] and R. HIDE [c]

[a] *Department of Physics (Atmospheric, Oceanic and Planetary Physics), Clarendon Laboratory, Parks Road, Oxford, OX1 3PU, U.K.;*
[b] *Meteorological Office, Met. Research Flight, Farnborough, Hants;*
[c] *Department of Physics (Atmospheric, Oceanic and Planetary Physics), Clarendon Laboratory, Parks Road, Oxford, OX1 3PU, U.K.*

(Received 12 July 1995; In final form 27 October 1997)

There have been extensive previous laboratory studies of thermal convection in a vertical cylindrical annulus of fluid that rotates about its axis with angular velocity $\mathbf{\Omega}$ (say) with respect to an inertial frame and is subject to an axisymmetric horizontal temperature gradient, as well as associated theoretical and numerical work. The relative flow produced by concomitant buoyancy forces is strongly influenced by Coriolis forces, which give rise to azimuthal circulations and promote, through the process of "baroclinic instability", regimes of non-axisymmetric sloping convection which can be spatially and temporally regular or irregular ("chaotic geostrophic turbulence"). It is also known from previous work that such flows are changed dramatically by the presence of a thin rigid impermeable radial barrier blocking the cross-section of the annulus, and capable of supporting a net azimuthal pressure gradient and associated net azimuthal temperature gradient within the fluid. The presence of the barrier can thus render convective heat transport across the fluid annulus (as measured by the Nusselt number, Nu) virtually independent of $\mathbf{\Omega}$ (as measured by the so-called Ekman or Taylor number) and dependent only on the Grashof number, G. The present study reports further systematic determinations of heat transport and of velocity and temperature fields in the presence of a radial barrier, with emphasis on the $\mathbf{\Omega}$-dependence of the crucially-important net azimuthal temperature gradient supported by the barrier and the physical interpretation of that dependence.

Keywords: Thermal convection; rotating fluid annulus; radial barrier

1. INTRODUCTION

The extent to which hydrodynamical motion in a fluid system is effected by the general rotation of the whole system with angular velocity $\mathbf{\Omega}$ relative to an inertial frame depends not only on the magnitude of $\mathbf{\Omega}$ but also *inter alia* on the shape and topological characteristics of the fluid container. Hide (see Appendix) considered the case when $\mathbf{\Omega}$ is independent of time t, the fluid density ρ (in general a function of t and position $\mathbf{r}$) is constant (and equal to $\bar{\rho}$), and inquired whether there were any circumstances in which the Eulerian flow velocity $\mathbf{u}(\mathbf{r}, t)$ was independent of $\mathbf{\Omega}$ and therefore the same when $\mathbf{\Omega} \neq \mathbf{0}$ as when $\mathbf{\Omega} = \mathbf{0}$ [i.e. $\mathbf{u}_0(\mathbf{r}, t)$]. He concluded that this situation could arise in a simply-connected system, such as the differentially heated rotating fluid annulus described in this paper. In this case, when $\mathbf{\Omega} \neq \mathbf{0}$ the fluid velocity may remain equal to $\mathbf{u}_0$ because of the appearance of an additional dynamic pressure field $p_1(\mathbf{r}, \Omega, t)$ which satisfies

$$2\bar{\rho}\,\mathbf{\Omega} \times \mathbf{u}_0 = -\nabla p_1, \tag{1}$$

where $p(\mathbf{r}, \Omega, t) = p_0(\mathbf{r}, t) + p_1(\mathbf{r}, \Omega, t)$ so that p_0 is the pressure field in the absence of rotation and p_1 arises as a consequence of rotational effects.

In the case of buoyancy-driven flows produced by the action of gravity, $\mathbf{g}$ on density gradients $\nabla\rho$ (maintained, for example, by differential heating, as in planetary atmospheres) one might expect advective processes such as heat transfer to be strongly influenced by the shape and topology of the container when Ω ($\equiv |\mathbf{\Omega}|$) is large. The investigation of such effects bears not only on the study of basic hydrodynamical processes in rotating fluids but also in the interpretation of observations of flows in natural rotating fluid systems such as the atmosphere and oceans. For it is a remarkable circumstance that the essential features of large-scale flows in atmospheres and oceans can be reproduced and studied on the much smaller scale of the laboratory (see e.g. Hide, 1977). In the present paper we shall be concerned with thermal convection in a rotating fluid annulus (see e.g. Hide and Mason, 1975) under conditions when the centripetal acceleration $\mathbf{\Omega} \times (\mathbf{\Omega} \times \mathbf{r})$ is very much smaller in magnitude than the

acceleration due to gravity **g**. In the first studies of such a system (Hide 1953, 1958), where the main objective was the delineation of various flow regimes and their dynamical characteristics (including non-uniqueness, chaotic and other essentially non-linear behaviour), and temperature fields, more or less incidental determinations were made of the dependence of radial heat transfer on Ω and the other impressed conditions. The Nusselt Number

$$\mathrm{Nu} \equiv \frac{H \ln (b/a)}{2\pi k \Delta T d} \tag{2}$$

(where H is the total heat transport by the fluid through the annulus, and the other quantities are defined in Tab. I) is a dimensionless measure of the total heat transfer (see e.g. Tritton, 1988; Kreith, 1968). Nu generally decreases with increasing Ω, more rapidly in the axisymmetric flow regime found at the lowest values of Ω covered by the experiments and in the non-axisymmetric regime of 'geostrophic-turbulence' found at the highest values, than in the regular non-axisymmetric flow regime found at intermediate values of Ω, in which the heat transport is more or less constant. A by-product of an attempt to give a theoretical interpretation of these results was a conjecture by Hide (see Appendix) that the addition of a rigid impermeable radial barrier connecting the inner and outer cylinders of the annular convection chamber at all levels might result in an Ω-dependent pressure field (p_1) sufficient to render Nu independent of Ω (and equal to its value at $\Omega = 0$). The conjecture was investigated and confirmed in work by Bowden (1961), using apparatus designed

TABLE I Range of experimental parameters

Radius of inner cylinder	a	2.5 cm
Radius of outer cylinder	b	8.0 cm
Depth of annular cavity	d	14.0 cm
Angular velocity	Ω	0.0 – 5.0 rad·sec^{-1}
Mean fluid temperature	$\bar{T}$	20°C
Applied temperature difference	ΔT	4 or 10°C
Kinematic viscosity of fluid	ν	$1.79 - 1.83 \times 10^{-2}$ cm·sec^{-1}
Specific heat capacity of fluid	C_p	3.84 – 3.85 J·g^{-1}·°C^{-1}
Mean density of fluid	$\bar{\rho}$	1 g·cm^{-3}
Expansion coefficient of fluid	α	3.03×10^{-4} °C^{-1}
Thermal conductivity of fluid	k	5.18×10^{-3} W·cm^{-1}·°C^{-1}

specifically for heat transfer measurements. Other work included studies of the influence of full and partial barriers on flow patterns and on the broad characteristics of the temperature field in the convecting fluid (Bowden and Eden, 1968; Bless, 1965; Rayer, 1992). Temperature measurements are particularly important, for they provide *inter alia* information about the pressure field (see Appendix) which in the laboratory studies cannot readily be determined by direct measurements.

Consistent with Hide's proposal, Bowden and Eden (1968) observed systematic azimuthal temperature gradients which increased in magnitude with increasing Ω, and they noticed the formation of horizontal eddies at the highest values of Ω used in their experiment. In the present paper we extend these studies with the objective of elucidating the mechanisms at work; particularly the role of the horizontal eddies.

2. APPARATUS

The apparatus used to obtain the measurements is essentially the same as that used by Hignett *et al.* (1985); Hide *et al.* (1977) and Hide and Mason (1975). It consists of two coaxial cylinders (with radii a and b) arranged so as to form an annular convection chamber, which was placed on a rotating turntable. The convection chamber was placed so that its central axis of symmetry coincided with the axis of rotation of the turntable. The turntable could be rotated with uniform angular velocity, Ω, between 0 and 5 rad.sec^{-1}. Fluid filled the cavity between these cylinders and a thermally insulating horizontal base and rigid lid.

The side walls of the annulus were held at different constant temperatures, T_a (the inner cylinder at $r = a$) and T_b (the outer cylinder at $r = b$), so that a radial temperature difference $\Delta T \equiv T_b - T_a$ with $T_b > T_a$ was applied across the fluid.

The experiments required that the annulus was fitted with a single fully blocking thermally insulating perspex radial barrier of thickness 2.5 mm, which blocked the entire radius and depth of the convection chamber at $\phi = \pm \pi$, so that the $\phi = 0$ position was located opposite it.

Fluid motions were visualized by a technique involving neutrally buoyant tracer particles, as described by Jonas and Kent (1979). The

fluid used was a water-glycerol mixture with a density of $\rho \approx 1\,\mathrm{g.cm}^{-1}$ at 20°C, which was seeded with small neutrally buoyant polystyrene beads. Horizontal beams of light were used to illuminate the flow field and thus allow the automatic computer tracking of the beads at a range of vertically displaced levels in the annulus.

Fluid temperature measurements were made at mid-radius $[r = (a+b)/2]$ and mid-depth ($z = 0$) by an azimuthal array of thirty-two equally spaced thermocouples. Measurements of the temperature change in the inner cylinder cooling fluid allowed the total heat transport through the convection chamber to be determined. The flow-field temperature data was used as a temporal mean, and all measurements were made with steady rotational and thermal forcing. The presence of the radial barrier in the rotating system was generally associated with a temperature drop across it, which was defined as

$$\Delta T_B \equiv T^{\mathrm{warm}} - T^{\mathrm{cool}},$$

where T^{warm} was the temperature of the warmest thermocouple in the ring at any given Ω, and T^{cool} the temperature of the coolest thermocouple. Separate apparatuses were used for the flow visualisation and heat transport measurements, these were identical apart from their instrumentation. The range of fluid properties and other parameters used in the experiments are given in Table I.

3. RESULTS WITH AN INSULATING RADIAL BARRIER

The measurements described here were obtained using an annulus with a flat base and the insulating barrier described in Section 2. Fowlis and Hide (1965) defined dimensionless parameters

$$\Theta \equiv \frac{g\alpha \Delta T d}{\Omega^2 (b-a)^2} \quad \text{and} \quad \tau \equiv \frac{4(b-a)^5 \Omega^2}{\nu^2 d},$$

where g is the acceleration due to gravity and the other symbols are defined in Table I. The experiments covered the ranges $2.2 \times 10^{-2} \leq \Theta \leq \infty$, $0 \leq \tau \leq 1.1 \times 10^8$, while eddies were observed for $\Theta \lesssim 0.4$ and $\tau \gtrsim 10^7$. Figure 1 shows the typical azimuthal temperature variation at

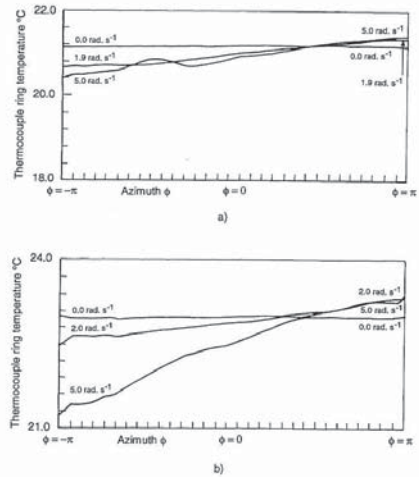

FIGURE 1 Experimental results showing temperature of ring thermocouple against azimuthal position for three rotation rates, $\Omega = 0.0$, 1.9 (or 2.0) and 5.0 rad.sec^{-1}, for the system with constant depth, $d = 140$ mm and the full thermally insulating barrier. Each of the scale markings along the horizontal axis shows the location of one of the thermocouples in the ring. Measurements of temperature were taken for each thermocouple in the ring, with a straight line drawn between them as a guide to the eye. The standard errors were 0.014 °C in both cases. The externally applied temperature differences were (a) $\Delta T \approx 4$ °C, (b) $\Delta T \approx 10$ °C. The $\Delta T_B(\Omega)$ was defined as the difference between the maximum and minimum thermocouple ring temperatures for a given Ω. As the figures show ΔT_B was generally the temperature difference between one side of the barrier and the other.

different rotation rates measured by the thermocouple ring at mid-radius ($r = \bar{r}$), and mid-height ($z = 0$) as a function of ϕ, $T(\bar{r}, z = 0; \phi, t)$. The barrier was placed at $\phi = \pm\pi$. Plots of temperature are given for three values of Ω for each of the two values of ΔT used. It can be seen that $\partial T(\bar{r}, z = 0; \phi)/\partial\phi \approx$ *constant* at a given rotation rate, although temperature perturbations appear at higher values of Ω in some cases. The temperature drop across the barrier, ΔT_B can be seen to increase with Ω.

The dependence of ΔT_B on Ω can be seen more clearly in Figure 2. It can be seen that for constant ΔT, ΔT_B increases approximately linearly with Ω before levelling off at a value of 20–25% of ΔT.

The total heat transport of the fluid as expressed by the Nusselt number (see equation 2), Nu(Ω) is shown in Figure 3. The results show that Nu (and therefore the radial heat transport by the fluid) remains fairly constant with Ω, at approximately the same value as when $\Omega = 0$. At $\Delta T = 10\,^{\circ}\mathrm{C}$ the largest value of Nu is still only about 7% above the $\Omega = 0$ value.

Typical velocity measurements are shown in Figures 4 to 7. Figures 4, 5 and 7 show radial motions in opposite directions at the top and bottom of the annulus, which are consistent with a radial overturning cell with fluid rising by the warm outer cylinder, and sinking by the cool inner cylinder. Azimuthal motions can be seen in Figures 4 and 6; at mid-height there is prograde flow by the outer cylinder and retrograde flow by the inner cylinder. Figure 6 shows that the shear of this azimuthal flow tends to increase with Ω. There is also some variation of the azimuthal motion with height. At higher rotation rates smaller scale eddies were also seen, an example can be seen in Figure 7(c).

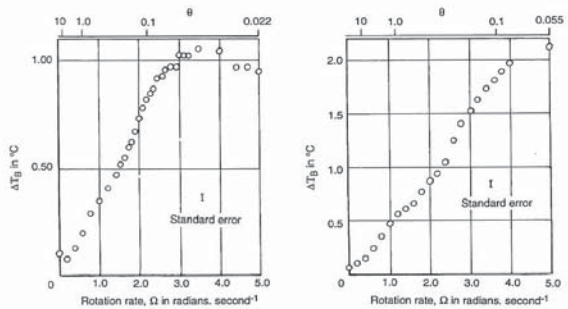

FIGURE 2 Experimental results showing dependence of ΔT_B on Ω, for the system with a full thermally insulating barrier and depth, $d = 140$ mm. The externally applied temperature differences were (a) $\Delta T \approx 4\,^{\circ}\mathrm{C}$ and (b) $\Delta T \approx 10\,^{\circ}\mathrm{C}$.

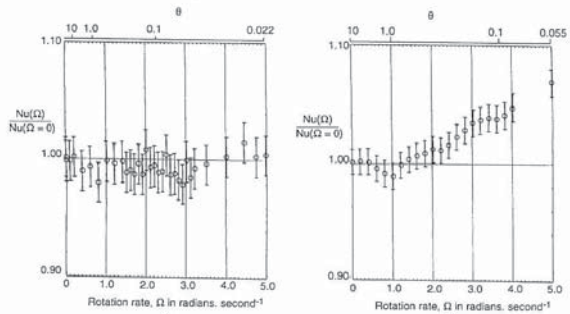

FIGURE 3 Experimental results showing the dependence of Nu(Ω)/Nu($\Omega = 0$) on Ω, for the system with a full thermally insulating radial barrier and depth, $d = 140$ mm. The externally applied temperature differences were (a) $\Delta T \approx 4\,^{\circ}\mathrm{C}$ and (b) $\Delta T \approx 10\,^{\circ}\mathrm{C}$.

The observations of the flow can be summarised as follows. The flow appears to consist of three main components: (1) a radial overturning, (2) a horizontal circulation (with some vertical structure), and (3) smaller scale eddies that appeared at higher values of Ω. A temperature drop, ΔT_B was observed across the barrier for all values of $\Omega \neq 0$. This ΔT_B appears to increase linearly with Ω until its maximum value of about 25% ΔT is reached. The total heat transported by the fluid remained close to the $\Omega = 0$ value.

4. DISCUSSION

In this section the aim is to determine whether the mechanism keeping Nu independent of Ω is that suggested by Hide (see Appendix), namely that rotation gives rise to a dynamic pressure field (p_1) with associated temperature field (T_1) which allows the fluid velocity field to be unaffected by rotation (i.e. $\mathbf{u} = \mathbf{u}_0$).

Excluding the smaller scale eddies, the interpretation of the experimental results can be considerably simplified by regarding the

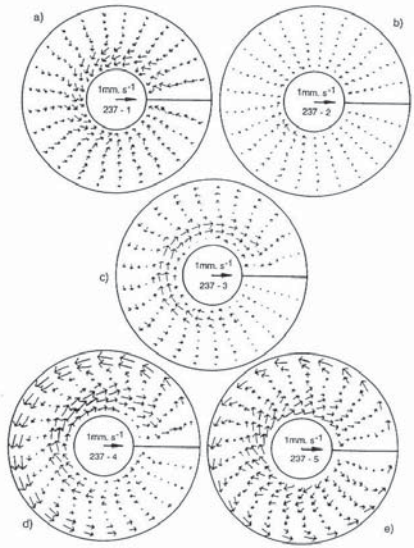

FIGURE 4 Horizontal velocity field data from the flow visualisation technique interpolated onto a regular grid, for the annulus with a full thermally insulating barrier. The location of the barrier is indicated by the solid line in the 3 o'clock position. The flow is shown at various heights above the base of the annulus, these are; (a) 124 mm, (b) 97 mm, (c) 70 mm, (d) 43 mm, and (e) 16 mm. Here $\Omega = 1.20$ rad.sec^{-1}, $\Delta T = 10.09\,^{\circ}$C, $\Theta = 9.5 \times 10^{-1}$, $\tau = 6.7 \times 10^{6}$. In each case the central arrow depicts a velocity of 1mm.sec^{-1}. The depth of the annulus was $d = 140$ mm.

fluid motions as a superposition of two circulations. These circulations are shown schematically in Figure 8. The first is a radial overturning cell, characterised by $\partial u/\partial z \approx constant$. The axis of this circulation lies antiparallel to $\hat{\boldsymbol{\phi}}$, the unit azimuthal vector, and by analogy with the components of the relative vorticity vector $\boldsymbol{\omega} = (\xi, \eta, \zeta)$ [where the components of the position vector $\mathbf{r} = (r, \phi, z)$] shall be denoted the η-circulation. The second circulation is assumed to be independent of z

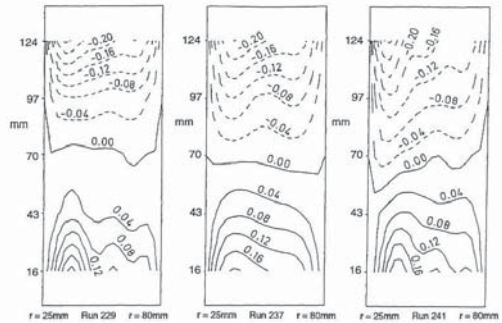

FIGURE 5 The figures show contours of the azimuthal mean of the radial component of velocity in an (r, z) plane, for the system with an insulating barrier and constant depth, $d = 140$ mm. Solid contours represent radially outwards flow and dashed contours, inwards flow. (a) $\Delta T = 10.00\,^{\circ}$C, $\Omega = 0.400$ rad.sec^{-1}, $\Theta = 8.4$, $\tau = 7.5 \times 10^{5}$, (b) $\Delta T = 10.09\,^{\circ}$C, $\Omega = 1.196$ rad.sec^{-1}, $\Theta = 9.5 \times 10^{-1}$, $\tau = 6.7 \times 10^{6}$ and (c) $\Delta T = 9.98\,^{\circ}$C, $\Omega = 3.003$ rad.sec^{-1}, $\Theta = 1.5 \times 10^{-1}$, $\tau = 4.2 \times 10^{7}$. In all cases a clear shear of radial velocity with z can be seen, which is suggestive of radial overturning. In (b) and (c) the even spacing of the contours with z at mid-radius indicates that $\partial u/\partial z \approx constant$.

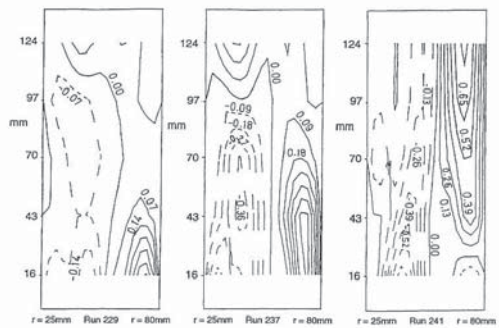

FIGURE 6 The figures show contours of the mean over ϕ of v in an (r, z) plane for the annulus with a full insulating barrier and depth, $d = 140$ mm. Solid contours represent prograde flow and dashed contours retrograde flow. The cases (a)–(c) correspond to those of Figure 5. The flow patterns appear to be quite complex with both radial and vertical shear. At mid-height ($z = 0$) the shear of v appears to increase with Ω.

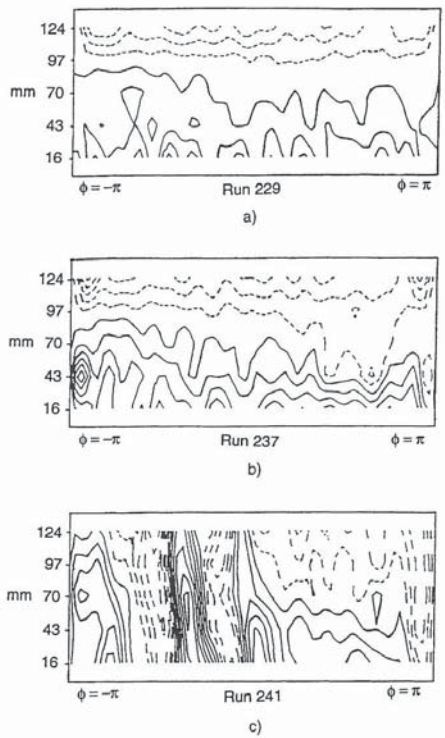

FIGURE 7 The figures show contours of u in a (ϕ, z) plane for the annulus with a full insulating barrier. Solid contours represent radially outwards flow and dashed contours, inwards flow. The cases (a)–(c) correspond to those of Figure 5. The contour intervals are (a) 0.08 mm.sec^{-1}, (b) 0.07 mm.sec^{-1} and (c) 0.12 mm.sec^{-1}.

and lies in a horizontal plane. Using the same thinking as above it shall be known as the ζ-circulation. While there is evidence (Fig. 6) that the ζ-circulation is not independent of z, the contribution it makes to fluid

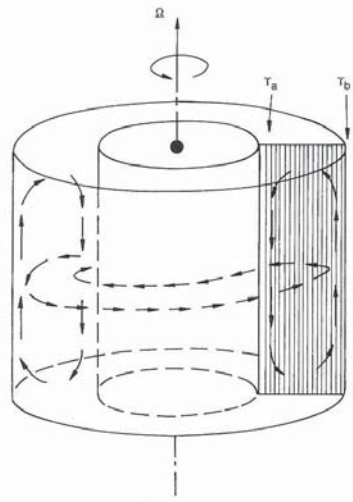

FIGURE 8 Diagram illustrating the simplified flow pattern representing fluid motions for the results described in Section 4. The velocity measurements when there are no eddies are represented by the two circulations shown by the arrows. The radial overturning cell, which is independent of ϕ, is called the η-circulation, while the horizontal circulation, which is independent of z is called the ζ-circulation. These circulations represent a useful simplification to the observed flows when eddies are absent. From Rayer (1994).

heat transfer is estimated to be quite small (Section 4.4) and the assumption represents a useful simplification in the following theory.

Both these circulations contribute to radial motions in the fluid (the radial motion in the ζ-circulation being restricted to close to the barrier), and so may contribute to radial heat transport by the fluid. By using this simplification the problem of understanding how the fluid maintains the heat transport reduces to that of finding mechanisms for the two circulations, and the heat transport contributions of each of the circulations and the eddies.

4.1. Heat Transport Considerations

The experiments measured the total heat transported by the fluid, $H = H_{\text{cond}} + H_{\text{adv}}$, where $H_{\text{cond}} = 2\pi k \Delta T d/\ln(b/a)$ is the heat transport through the fluid by conduction, and H_{adv} is the heat transport by advection. Thus the advective heat transport is obtained by subtracting the conductive heat transport from H. The net heat transport through a surface $\mathcal{S}$ by advection is

$$H_{\text{adv}}(r, \phi, z, t) = \int_{\mathcal{S}} \boldsymbol{H}_{\text{adv}}(r, \phi, z, t) \cdot d\boldsymbol{\mathcal{S}}, \tag{3}$$

hence if the temperature and velocity fields for the fluid motions are known, H_{adv} may be calculated from them for comparison with the experimental results. In practice it was not possible to measure the entire temperature field, $T(r, \phi, z, t)$, and the velocity field data was limited by its accuracy. The approach followed for the temperature field was to use the limited data available, $T(\bar{r}, z = 0; \phi, t)$ with appropriate approximations. The velocity field data was used to identify the qualitative features of the flow, so that fluid velocities could be calculated using appropriate theory, from the more accurate temperature field data and various experimental parameters. It proved possible to identify the mechanism for the η-circulation, however the nature of the ζ-circulation was such that velocity data had to be used to estimate its heat transport contribution.

The total advective heat transport is given by (3) where $\mathbf{H}_{\text{adv}} = \rho C_p \mathbf{u} T$ and the direction of $d\boldsymbol{\mathcal{S}}$ is normal to the surface $\mathcal{S}$. If the lid and base of the annulus were perfect insulators, the heat advected through the annulus (and measured at the inner cylinder) must have passed through a cylindrical surface of height d at mid-radius, $\bar{r} = (a + b)/2$. In this case the normal to the surface is parallel to $\hat{\mathbf{r}}$, the unit vector in the r-direction, so that $d\boldsymbol{\mathcal{S}} = \hat{\mathbf{r}} \bar{r} d\phi dz$. As $\mathbf{u} = (u, v, w)$, u denotes the radial component of velocity so that the advective heat transport may be written

$$H_{\text{adv}}(\bar{r}; \phi, z, t) = \int_{\phi_0}^{\phi_1} \int_{z_0}^{z_1} \rho(\bar{r}; \phi, z, t) C_p(\bar{r}; \phi, z, t) \, u(\bar{r}; \phi, z, t) T(\bar{r}; \phi, z, t) \, dz \, \bar{r} \, d\phi. \tag{4}$$

Equation (4) is to be integrated between

$$\phi_0 = -(\pi - \varepsilon), \ \phi_1 = \pi - \varepsilon, \ z_0 = -\frac{d}{2}, \ z_1 = \frac{d}{2}, \tag{5}$$

where 2ε is the angular thickness of the barrier.

Next assume the density and specific heat of the fluid to be constant and equal to $\bar{\rho}$ and $\bar{C}_P$, where the overbar denotes the spatial average over the fluid. The values for $\bar{\rho}$ and $\bar{C}_P$ were taken to be the fluid density and the specific heat capacity of a water-glycerol solution of that density at 20°C.

The temperature may be written

$$T(\bar{r}; \phi, z, t) = \frac{\Delta T_\phi(\bar{r}, z = 0; t)}{2\pi} \phi + \frac{\Delta T_z(\bar{r}, \phi = 0; t)}{d} z + T'(\bar{r}; \phi, z, t) + \bar{T}, \tag{6}$$

where it should be noted that subscripts are not (and shall not be) used to represent derivatives. By definition $\Delta T_\phi(\bar{r}, z = 0; t)$ and $\Delta T_z(\bar{r}, \phi = 0; t)$ are independent of ϕ and z respectively, though not of t. The ΔT_ϕ and ΔT_z have been formulated so that they correspond to the (potentially) measurable quantities of the azimuthal and vertical temperature differences in the fluid. Equation (6) is formally correct because $T'(\bar{r}; \phi, z, t)$ is a completely general function of ϕ, z and t. However the first two terms (linear in ϕ and z) have been chosen because they represent a useful approximation to the temperature field in the analysis that follows. In the analysis $\bar{T}$ should be defined in the same way as $\bar{\rho}$ above, however experimental constraints meant that in practice the azimuthal average of T was used to calculate $\bar{T}$ when its value was required.

A further simplification is made by using

$$T'(\bar{r}; \phi, z, t) \approx T'(\bar{r}, z = 0; \phi, t). \tag{7}$$

This is done because the thermocouple ring data gives $T(\bar{r}, z = 0; \phi, t)$ so while there is no prospect of being able to calculate any z dependence in T' it might be possible to calculate the ϕ dependence. A further consideration is that the temperature perturbations that appear in the thermocouple ring data at certain rotation rates [e.g. see

Fig. 1(a)] show that there are at least non-linearities in the ϕ dependence of T'. Using the approximations above, assuming that the fluid is incompressible and making use of the fact that the walls of the annulus are not porous, (4) may be rewritten

$$H_{\text{adv}}(\bar{r};\phi,z,t) = \bar{\rho}\bar{C}_p \int_{\phi_0}^{\phi_1}\int_{z_0}^{z_1} u(\bar{r};\phi,z,t)[T(\bar{r};\phi,z,t)-\bar{T}]\,dz\,\bar{r}\,d\phi. \tag{8}$$

If the flow is split into the two circulations suggested in Section 4 and illustrated in Figure 8, then $u(\bar{r},\phi,z,t)$ may be written

$$u(\bar{r};\phi,z,t) = u_\eta(\bar{r};z,t) + u_\zeta(\bar{r};\phi,t) + u'(\bar{r};\phi,z,t), \tag{9}$$

where $u_\eta(\bar{r};z,t)$ represents the radial velocity at $r=\bar{r}$ due to the η-circulation and $u_\zeta(\bar{r};\phi,t)$ is the radial velocity due to the ζ-circulation. Then $u'(\bar{r};\phi,z,t)$ represents any other flows that may be present in the fluid, and in particular will include the small scale eddies seen at higher values of Ω. Since $u'(\bar{r};\phi,z,t)$ is a perfectly general function of ϕ, z and t, (9) is formally correct. Thus $H_{\text{adv}}(\bar{r};\phi,z,t)$ may be written as the sum of $H_\eta(\bar{r};\phi,z,t)$, the heat advected by the η-circulation; $H_\zeta(\bar{r};\phi,z,t)$, is the heat advected by the ζ-circulation and $H'(\bar{r};\phi,z,t)$ is the heat advected by any other processes, including the eddies. Hence H_η, H_ζ and H' may be defined as

$$H_\eta(\bar{r};\phi,z,t) \equiv \bar{\rho}\bar{C}_p \int_{\phi_0}^{\phi_1}\int_{z_0}^{z_1} u_\eta(\bar{r};z,t)[T(\bar{r};\phi,z,t)-\bar{T}]\,dz\,\bar{r}\,d\phi, \tag{10}$$

$$H_\zeta(\bar{r};\phi,z,t) \equiv \bar{\rho}\bar{C}_p \int_{\phi_0}^{\phi_1}\int_{z_0}^{z_1} u_\zeta(\bar{r};\phi,t)[T(\bar{r};\phi,z,t)-\bar{T}]\,dz\,\bar{r}\,d\phi, \tag{11}$$

and

$$H'(\bar{r};\phi,z,t) \equiv \bar{\rho}\bar{C}_p \int_{\phi_0}^{\phi_1}\int_{z_0}^{z_1} u'(\bar{r};\phi,z,t)[T(\bar{r};\phi,z,t)-\bar{T}]\,dz\,\bar{r}\,d\phi. \tag{12}$$

Each of these terms is discussed below. In the case of the η-circulation it has been possible to propose a mechanism, so that an expression for $u_\eta(\bar{r};z,t)$ can be derived. The measurements described in the present paper did not indicate a mechanism to account for H_ζ and H' and so only their advective heat transport contributions are discussed (however see Rayer, 1994 and Section 4.4 for a possible explanation of the mechanism for the ζ-circulation).

4.2. Suggested mechanism for the η-circulation

Following Hide's suggestion (see Appendix), the approximately linear dependence of u on z shown in Figure 5 and the appearance of a temperature drop across the barrier suggest that $u_\eta(\bar{r};z,t)$ may be governed by a balance between the Coriolis force and an azimuthal pressure gradient supported by the barrier. As the azimuthal pressure gradient arises from rotational effects in the fluid, equation (1) applies. In this case the equation for hydrostatic balance

$$\frac{1}{\bar{\rho}}\frac{\partial p}{\partial z} \approx -\alpha g(T-\bar{T})+g$$

(where $\bar{\rho}$ and $\bar{T}$ are the mean fluid density and temperature, and p is the pressure) may be used to eliminate p from equation (1). Thus following the notation of Section 1, where subscript '0' refers to the values of $\mathbf{u}, p, T$ when $\Omega = 0$, and subscript '1' to the additional components of $\mathbf{u}, p, T$ which arise from rotational effects (so that when $\Omega \neq 0, \mathbf{u} = \mathbf{u}_0 + \mathbf{u}_1$, $T = T_0 + T_1$, etc.), and using $\theta_1 = -\alpha T_1$ gives

$$\frac{\partial u_0}{\partial z}(\bar{r};\phi,z,t) \approx -\frac{g\alpha}{2\Omega\bar{r}}\frac{\partial T_1}{\partial \phi}(\bar{r};\phi,z,t).$$

Integration then yields

$$u_0(\bar{r};\phi,z,t) \approx \frac{-g\alpha}{2\Omega\bar{r}}\int_z \frac{\partial T_1}{\partial \phi}(\bar{r};\phi,z,t)dz + u_c(\bar{r};\phi,t),$$

where $u_c(\bar{r};\phi,t)$ is the function of integration. Since $\partial T_0/\partial\phi = 0$ any ϕ-dependence in T arises because of T_1, thus $\partial T/\partial\phi = \partial T_1/\partial\phi$ so that using (6) and (7), and expressing u_c as the sum of $\acute{u}(\bar{r};\phi,t)$ (which is

linear in ϕ) and $\tilde{u}(\bar{r};\phi,t)$ (which is a completely general function of ϕ) means that $u(\bar{r};\phi,z,t)$ can be rewritten

$$|u_0(\bar{r};\phi,z,t)| \approx \frac{g\alpha}{2\Omega\bar{r}}\int_z \frac{\Delta T_\phi(\bar{r},z=0;t)}{2\pi}\,dz + \acute{u}(\bar{r};\phi,t) + \left[\frac{g\alpha}{2\Omega\bar{r}}\int_z \frac{\partial T'}{\partial\phi}(\bar{r},z=0;\phi,t)\,dz + \tilde{u}(\bar{r};\phi,t)\right], \tag{13}$$

where the minus sign has been removed by considering $|u_0|$, its effect being to indicate that heat advection was radially inwards, towards the centre of the annulus. Since we are looking for flows in which $u(\bar{r};\phi,z,t) = u_0(\bar{r};\phi,z,t)$ comparison with (9), noticing that the first term on the right-hand side of (13) is a function of $(\bar{r};z,t)$ shows that

$$|u_\eta(\bar{r};z,t)| \approx \frac{g\alpha}{2\Omega\bar{r}}\int_z \frac{\Delta T_\phi}{2\pi}(\bar{r},z=0;t)\,dz\,. \tag{14}$$

In other words the mechanism of the η-circulation is that of a radial geostrophic overturning cell. Similarly the second term depends on $(\bar{r};\phi,t)$, so that $\acute{u}(\bar{r};\phi,t)$ is $u_\zeta(\bar{r};\phi,t)$, while the final term (in square brackets) expresses $u'(\bar{r};\phi,z,t)$. The implication is that when $u_c(=\acute{u}+\tilde{u})$ and $\partial T'/\partial\phi = 0$, $u_0 = u_\eta$.

Now $H_\eta(\bar{r};\phi,z,t)$ can be obtained by substituting (14) and (6) into (10), and integrating over z and ϕ, using the limits in (5). Since the half-angular thickness of the barrier $\varepsilon \ll \pi$ it can be neglected, also since there was no data available for $\Delta T_z(\bar{r},\phi=0;t)$, the approximation was made that $\Delta T_z \approx \Delta T$. The work of Hide and Mason (1975) tended to suggest that $\Delta T_z \sim (1/2)\Delta T$ for unblocked annulus flows, thus the assumption that $\Delta T_z \approx \Delta T$ (required for the analysis that follows) suggests that an increased vertical temperature gradient in the fluid arises as one on the effects of the barrier on the flow. Further, putting $\Delta T_\phi = \Delta T_B$ means that $H_\eta(\bar{r};t)$ can now be expressed only in terms of experimental parameters and fluid properties:

$$H_\eta(\bar{r};t) \approx \frac{\bar{\rho}\bar{C}_p g\alpha\Delta T_B \Delta T d^2}{24\Omega}. \tag{15}$$

If it is possible to find a region of parameter space where the η-circulation is the primary cause of heat advection in the system, then it

should be possible to test the result of (15) explicitly. If such a region can be found then in it, $H_{\text{adv}} \approx H_\eta$ and $u_0 \approx u_\eta$ so that (1) is approximately satisfied and since $u \approx u_0$ then $\text{Nu}(\Omega \neq 0) \approx \text{Nu}(\Omega = 0)$ in agreement with Hide's conjecture.

4.3. Testing the Theory for the η-Circulation

If heat advection by small scale eddies forms the main contribution to $H'(\bar{r};\phi,z,t)$, then at values of Ω where no eddies form ($\Omega \lesssim 1.2\,\text{rad.sec}^{-1}$), $H'(\bar{r};\phi,z,t) \approx 0$. Also Figure 6 suggests that the ζ-circulation is weakest at small Ω. Therefore it is possible to make the hypothesis that at small Ω, the η-circulation dominates the heat advection, so that

$$H_{\text{adv}}(\bar{r};\phi,z,t) \approx H_\eta(\bar{r};t)$$

If this is the case, then by (15) we have

$$H_{\text{adv}}(\bar{r};t) \approx \frac{\bar{\rho}\bar{C}_p g\alpha\Delta T_B\Delta T d^2}{24\Omega}. \tag{16}$$

Rearranging (16) suggests defining the quantity

$$A_* \equiv \frac{24\Omega H_{\text{adv}}(\bar{r};t)}{\bar{\rho}\bar{C}_p g\alpha\Delta T_B\Delta T d^2}.$$

Thus when $A_* = 1$, heat advection is consistent with a radial geostrophic overturning satisfying Hide's conjecture. Figure 9 shows plots of A_* against Ω for the two values of ΔT used in the experiments. It can be seen that for $\Omega \lesssim 3.0$ rad. sec^{-1}, when $\Delta T = 4\,^\circ\text{C}$, $A_* \approx 1.15$. A similar value is found for $\Delta T = 10\,^\circ\text{C}$, but over a larger range of Ω. Only at quite large rotation rates in Figure 9(a) does A_* deviate significantly from unity, which is to be expected as the heat advection from the ζ-circulation and the eddies become more important at higher Ω. This deviation of A_* from unity corresponds to regions of parameter space where $u \neq u_0$ and Hide's conjecture no longer applies. The interpretation of A_* can be assisted by noticing that $A_* \approx H_{\text{adv}}/H_\eta$.

This result agrees closely with the hypothesis made above, namely that only the η-circulation makes a significant contribution to the heat

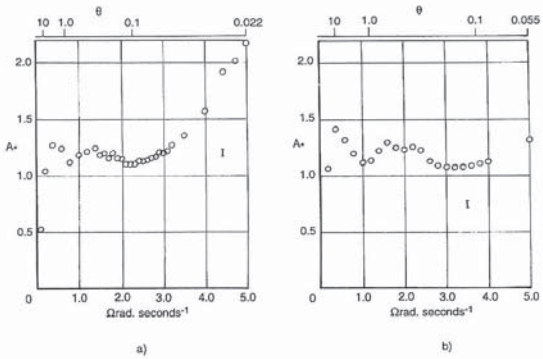

FIGURE 9 Plots of the dimensionless quantity A_* (see text) against Ω for the system with a full thermally insulating barrier and depth $d = 140$ mm. (a) $\Delta T = 4\,^{\circ}\mathrm{C}$, A_* appears to be of order unity for Ω less than about 3.0 rad.sec^{-1} and then increases fairly linearly with Ω at higher rotation rates. (b) $\Delta T = 10\,^{\circ}\mathrm{C}$, A_* remains of order unity over the range of Ω shown.

advection at low rotation rates ($\Omega \lesssim 3.0$ rad.sec^{-1}), and provides strong evidence that (15) correctly describes heat advection by the η-circulation.

The simple linear dependence of A_* on Ω for higher rotation rates in Figure 9(a) allows A_*^{-1} to be expressed empirically as

$$A_*^{-1} = A\,\mathrm{Min}(1,\, R_D/R), \tag{17}$$

where the function 'Min(x, y)' is defined as the smaller of the two quantities x and y, and

$$R_D \equiv \frac{\sqrt{g\alpha\Delta T d}}{2\Omega}. \tag{18}$$

Now R_D can be regarded as an estimate of the Rossby radius of deformation for the fluid. In this case we can write

$$Y(\bar{r};\,\Omega,\,t) = \frac{24\Omega H_{\mathrm{adv}}(\bar{r};\,t)\mathrm{Min}(1,\,R_D/R)}{\bar{\rho}\bar{C}_p\, g\alpha\Delta T d^2}\, A, \tag{19}$$

where it is to be expected that $Y \approx \Delta T_B$. Figure 10 shows plots of $Y(\bar{r};\Omega,t)$ against ΔT_B, where $A \sim 1$ and $R \sim 1$ cm. It can be seen that there is almost complete agreement to within the accuracy of the error bars. Thus $Y(\bar{r};\Omega,t)$ in (19) provides a very good estimate of ΔT_B if H_{adv} is known, or vice-versa.

A further test for the mechanism for the η-circulation can be seen from (14). By substituting ΔT_B for ΔT_ϕ in (14) and considering Figure 2 it can be seen that while $\Delta T_B \propto \Omega$, equation (14) predicts that $u_\eta(\bar{r};z,t)$ should be independent of Ω; up to about 3.0 rad. sec^{-1} in the $\Delta T = 4\,^{\circ}\mathrm{C}$ case, and for a greater range when $\Delta T = 10\,^{\circ}\mathrm{C}$. This observation is supported by Figure 5 where this does indeed appear to be the case and closer examination of fluid velocities showed that this was true, to the accuracy of the measurements; a further piece of evidence that (14) correctly describes $u_\eta(\bar{r};z,t)$.

4.4. Heat Advection by the ζ-Circulation

Equation (11) gives the heat advection by the ζ-circulation, $H_\zeta(\bar{r};\phi,z,t)$. Rayer (1994) has provided evidence that the ζ-circulation

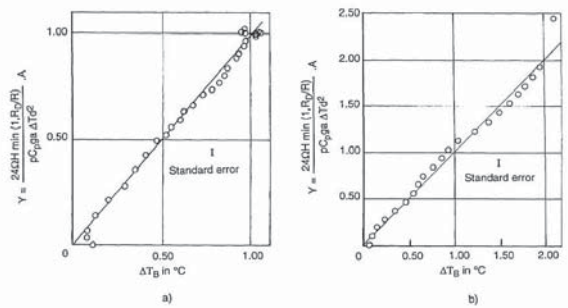

FIGURE 10 Plots of the quantity Y against experimental measurements of ΔT_B, for the system with a full thermally insulating barrier and depth, $d = 140$ mm. In both cases the results fall closely onto a straight line of gradient unity, indicating that $\Delta T_B \approx Y$ over the range shown. For (a) $\Delta T = 4\,^{\circ}\mathrm{C}$, $A = 0.85$, $R = 0.71$ cm and (b) $\Delta T = 10\,^{\circ}\mathrm{C}$, $A = 0.87$, $R \leq 0.64$ cm.

arises because of the effect of radial geostrophic balance on small radial temperature gradients in the fluid. However, since measurements of the radial dependence of temperature were not available, this does not allow $u_\zeta(\bar{r};\phi,t)$ to be calculated from the temperature field. However $H_\zeta(\bar{r};\phi,z,t)$, can still be estimated from experimental measurements of velocity. If $u_\zeta(\bar{r};\phi,t)$ is assumed to have a linear dependence on ϕ, then

$$u_\zeta(\bar{r};\,\phi,\,t) = \frac{\Delta u_\phi(\bar{r},z=0;t)}{2\pi}\phi,$$

so that substitution into (11) and integration over the limits in (5) gives

$$H_\zeta(\bar{r};\,\phi,\,t) = \frac{\bar{\rho}\bar{C}_p\Delta u_\phi(\bar{r},\,z=0;\,t)\bar{r}d}{2\pi}\left[\frac{\Delta T_\phi(\bar{r},\,z=0;\,t)\pi^2}{3} + \int_{\phi_0}^{\phi_1} T'(\bar{r},\,z=0;\,\phi,\,t)\,\phi\,d\phi\right], \tag{20}$$

assuming that the angular half-width of the barrier $\varepsilon \ll \pi$. As before, put $\Delta T_\phi \approx \Delta T_B$, and $\int T'(\bar{r},z=0;\phi,t)\,\phi\,d\phi$ can be calculated from the thermocouple ring measurements, $T(\bar{r},z=0;\phi,t)$. The Δu_ϕ was estimated from experimental velocity measurements.

As the measurements of v were perpendicular to the flow in the η-circulation, they can only arise from the ζ-circulation. Figure 11 shows plots of v against Ω, from where it can be seen that

$$|v| \approx 0.02\Omega \text{ cm.sec}^{-1} \quad \text{at} \quad \Delta T \approx 4\,^\circ\text{C},$$

and

$$|v| \approx 0.03\Omega \text{ cm.sec}^{-1} \quad \text{at} \quad \Delta T \approx 10\,^\circ\text{C}.$$

Using the equation for incompressible flow ($\nabla \cdot \mathbf{u} = 0$), and making use of the fact that $w \ll u, v$;

$$\frac{1}{r}\frac{\partial(ru)}{\partial r} + \frac{1}{r}\frac{\partial v}{\partial\phi} \approx 0, \Rightarrow u \approx -\frac{1}{r}\int\frac{\partial v}{\partial\phi}dr + \frac{u_\epsilon(\phi,\,z,\,t)}{r}.$$

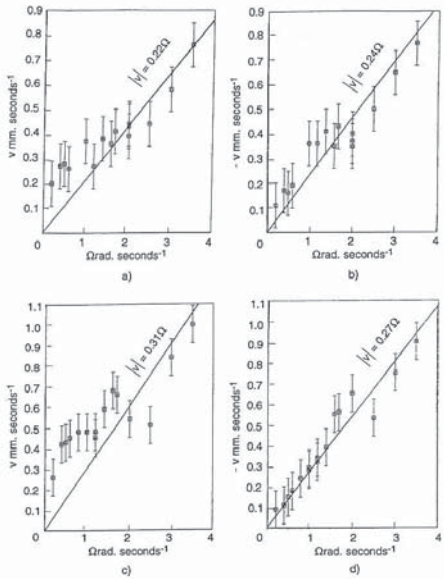

FIGURE 11 Plots of (a), (c) maximum positive v against Ω, (b), (d) maximum negative v against Ω, for (a), (b) $\Delta T = 4\,^\circ$C and (c), (d) $\Delta T = 10\,^\circ$C. Also plotted are solid lines showing (a), (b) $v = 0.2\,\Omega$ mm.sec^{-1}, and (c), (d) $v = 0.3\Omega$ mm.sec^{-1}.

It suggests that

$$\Delta u_\phi(\Delta T \approx 4\,^\circ\text{C}) \approx \frac{1}{\bar{r}}\cdot\frac{0.02\Omega}{2\pi}\cdot(b-a) = \frac{0.11\,\Omega}{2\pi\bar{r}}$$

and

$$\Delta u_\phi(\Delta T \approx 10\,^\circ\text{C}) \approx \frac{1}{\bar{r}}\cdot\frac{0.03\Omega}{2\pi}\cdot(b-a) = \frac{0.17\Omega}{2\pi\bar{r}}.$$

Thus (20) can be written

$$H_\zeta(\bar{r}, \Delta T \approx 4\,^\circ\mathrm{C}; \phi, t) = \frac{0.11\bar{\rho}\bar{C}_p\Delta T_B\Omega d}{12} + \frac{0.11\bar{\rho}\bar{C}_p\Omega d}{4\pi^2}\int_{\phi_0}^{\phi_1} T'\phi\, d\phi,$$

$$H_\zeta(\bar{r}, \Delta T \approx 10\,^\circ\mathrm{C}; \phi, t) = \frac{0.17\bar{\rho}\bar{C}_p\Delta T_B\Omega d}{12} + \frac{0.17\bar{\rho}\bar{C}_p\Omega d}{4\pi^2}\int_{\phi_0}^{\phi_1} T'\phi\, d\phi. \tag{21}$$

Estimates of the error in H_ζ were obtained by taking the steepest and shallowest slopes of the linear fit used to describe $|v|$ in Figure 11; these gave an error of 15% when $\Delta T \approx 4\,^\circ$C and 17% for $\Delta T \approx 10\,^\circ$C. It should be noted that since the maximum positive and negative values of v have been used, (21) is more likely to be an over estimate of H_ζ than an under estimate. Clearly if a possible overestimate of H_ζ is unable to account for the discrepancy between H_η and the measurements (H_{adv}) then some additional mechanism for heat transport is required. Values for $H_\zeta(\bar{r}; \phi, t)$ are plotted in Figure 12, along with the heat advection contributions of the η-circulation, and the total advective heat transport as measured by the experiments. Now H_ζ corresponds to heat transport in the same direction as H_η, though as can be seen, over all rotation rates, the estimates of H_ζ contribute significantly less to the total heat transport than H_η.

The estimates of fluid heat transfer by the ζ-circulation were made on the basis that it was independent of z, which represented a useful simplification for the theory that followed. Figure 6 suggests that this is perhaps an over-simplification, however as the calculations above indicate, the strength of the ζ-circulation coupled with the magnitude of the azimuthal temperature gradient in the fluid show that it transports much less heat than the η-circulation. This result seems unlikely to be significantly altered by using a more complex velocity profile for the ζ-circulation in the above theory.

4.5. Heat Advection by Small Scale Eddies

The heat advection by the small scale eddies is given by (12). As $u'(\bar{r}; \phi, z, t)$ could not be measured for $\Omega \{\gtrsim\} 3.0$ rad.sec^{-1}, due to the limitations of the velocity measurement apparatus, all that could be done was to estimate the order of magnitude of $H'(\bar{r}; \phi, z, t)$ when eddies were present. Another problem was that velocity and temperature measurements could not be made simultaneously, so that it was not possible to correlate the velocity and temperature measurements for the eddies. Figure 7(c) can be used to estimate the radial velocity shear with ϕ of an eddy as $\Delta u_E \sim 0.84$ mm.sec^{-1} at $\Omega = 3.0$ rad.sec^{-1} and $\Delta T \approx 10\,^\circ$C. At the same values of Ω and ΔT

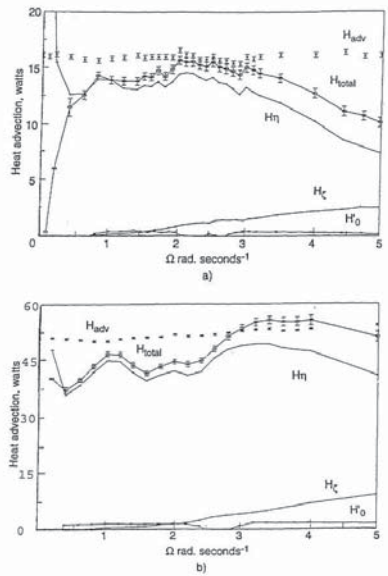

FIGURE 12 Plots showing the heat transport contributions for the insulating barrier. Heat transport contributions have been calculated for; the η-circulation, H_η, using (15); the ζ-circulation, H_ζ, using (21); and H'_0, using (22). $H_{\mathrm{total}} = H_\eta + H_\zeta + H'_0$. Experimental measurements of the advective heat transport, H_{adv} are shown for comparison. (a) $\Delta T \approx 4\,^\circ$C, (b) $\Delta T \approx 10\,^\circ$C. The lines serve only as a guide to the eye.

temperature measurements gave the difference between the maximum and minimum values of T' (eqn. 6), $\Delta T'$ as 0.530 °C. Also as the eddy in Figure 7(c) only occupies about one-fifth of the azimuth, $\delta\phi \sim 2\pi/5$. So that the *maximum* amount of heat the eddy could carry (if u' and T' were suitably correlated) would be

$$H'(\bar{r};\phi,z,t) \sim \bar{\rho}\bar{C}_p \Delta u_E \Delta T' \bar{r} d \frac{2\pi}{5} = 17 \text{ watts}.$$

Comparison with Figure 12 indicates that the eddy was not carrying that much heat, suggesting that u' and T' were not well correlated in this case. However the calculation does indicate that eddies can carry significant amounts of heat, and suggests that the eddies might be responsible for the increase in Nu seen in Figure 3(b), which does seem to occur for $\Omega \gtrsim 1.6$ rad.sec^{-1}, which is the same as the transition for the onset of the small scale eddies at $\Delta T \approx 10$ °C.

In an attempt to explore the heat advection by eddies a little further, (13) implies that

$$u'(\bar{r};\phi,z,t) \approx \frac{g\alpha}{2\Omega\bar{r}} \int_z \frac{\partial T'}{\partial \phi}(\bar{r}, z=0;\phi,t)dz + \tilde{u}(\bar{r};\phi,t),$$

where $\tilde{u}(\bar{r};\phi,t)$ is non-linear in ϕ. Now $H'(\bar{r};\phi,z,t)$ is given by (12). Though the mechanism for $\tilde{u}(\bar{r};\phi,t)$ remains unknown, it is possible to write

$$H'(\bar{r};\phi,z,t) = H'_0(\bar{r};\phi,z,t) + H'_1(\bar{r};\phi,z,t),$$

where

$$H'_0(\bar{r};\phi,z,t) \approx \bar{\rho}\bar{C}_p \int_{\phi_0}^{\phi_1} \int_{z_0}^{z_1} \frac{g\alpha}{2\Omega\bar{r}} \int_z \frac{\partial T'}{\partial\phi}(\bar{r}, z=0;\phi,t)\,dz \\ [T(\bar{r};\phi,z,t) - \bar{T}]\,dz\,\bar{r}\,d\phi.$$

Substitution from (6) for $T(\bar{r};\phi,z,t)$, and integration over ϕ using the limits given in (5) gives, using $\Delta T_z \approx \Delta T$,

$$H'_0(\bar{r};\phi,t) \approx \frac{\bar{\rho}\bar{C}_p g\alpha \Delta T d^2}{24\Omega} \int_{\phi_0}^{\phi_1} \frac{\partial T'}{\partial\phi}(\bar{r}, z=0;\phi,t)\,d\phi. \qquad (22)$$

Values of $H'_0(\bar{r};\phi,t)$ were calculated by integrating $\partial T'/\partial\phi$ around the thermocouple ring, and are plotted along with the other heat transport contributions in Figure 12. It can be seen that the values of H'_0 are rather small, and probably form only a tiny part of $H'(\bar{r};\phi,z,t)$. Equation (13) indicates that H'_0 is the correction that should be applied to (14) to allow for variations in the strength of the η-circulation with ϕ due to non linearities in $\partial T/\partial\phi$. As H'_0 is so small, clearly such corrections are not very important. Consequently it appears that the important contributions to $u'(\bar{r};\phi,z,t)$ are made by $\tilde{u}(\bar{r};\phi,t)$, an idea that is supported by Figure 7(c) which shows $u(\bar{r};\phi,z,t)$ to have a much stronger dependence upon ϕ than on z in the region of the eddy.

5. CONCLUSIONS

Section 3 gives a summary of the experimental results. It seems that the flow pattern observed may be regarded as a superposition of two circulations (see Section 4), the η and ζ-circulations, plus small scale eddies at higher rotation rates.

Theory suggested that at $r = \bar{r}$ the r-component of the velocity for the η-circulation could be described by (14). Physically this represents a balance between the Coriolis force and an azimuthal pressure gradient supported by the barrier. The pressure drop across the barrier is associated with the temperature drop ΔT_B. Heat advection by the η-circulation is described by (15). At values of Ω less than 3.0 rad.sec^{-1} for $\Delta T = 4$°C, and over a larger range when $\Delta T = 10$°C the heat advection of the η-circulation gives a good approximation to the heat advection measured in the experiments. This appears to correspond to the case when the ζ-circulation and the small scale eddies transport little heat so that only the η-circulation contributes significantly to the heat advection by the fluid. In this range (19) provides a diagnostic equation that links the heat advection to ΔT_B through experimental parameters and fluid properties. Thus there is strong evidence that suggests that the η-circulation is correctly parameterized by (14) and (15) and described by the physical mechanism described above.

Further, (17)–(19) provide a set of empirically based diagnostic equations that link the heat advection to ΔT_B in a similar fashion, over the whole range of Ω covered in the experiments.

Velocity measurements have allowed the heat advection of the ζ-circulation to be estimated by (21). Estimates of heat advection by small scale eddies suggest that they may play a significant role in heat advection when present.

Figure 12 shows the heat advection contributions of the various processes described above. While these mechanisms do seem to account for the bulk of the measured heat advection, there are still regions where the discrepancy is greater than the error bars. At the very smallest values of Ω this may be because geostrophic balance in the ϕ-direction is no longer valid, so that (13) is no longer appropriate. At large values of Ω it seems likely that eddies will play an increasingly important role in heat advection. However a weakness in the theory is that $\partial T/\partial\phi$ has been assumed to be independent of z, and ΔT_z has not been measured at all, this may also be the cause of the less good agreement at smaller values of Ω. A further consideration is the possible contribution to heat transport by flow in the boundary layers that form on the sides of the barrier, such boundary layers will be highly non-geostrophic and as no boundary layer measurements were taken, have not been considered in the current work.

Despite these problems there is sufficient agreement between the theory and the measurements to suggest that the mechanisms keeping the heat advection (and therefore Nu) close to its non-rotating value over the range of Ω are as follows.

At low to medium rotation rates ($\Omega \lesssim 3.0$ rad.sec^{-1} at $\Delta T = 4°$C, and $\Omega \lesssim 4-5$ rad.sec^{-1} at $\Delta T = 10°$C) heat is advected mainly by the η-circulation, at a rate which is independent of Ω so long as $\Delta T_B \propto \Omega$ [see equation (15)]. This corresponds to the case suggested by Hide in the Appendix and given in equation (1), where the force on a fluid particle due to the azimuthal gradient of the dynamic pressure field balances the Coriolis force on the particle, so that radial fluid motions occur with their accompanying heat advection. The heat advection by the ζ-circulation is insignificant as ΔT_B is rather smaller than $\Delta T_z \approx \Delta T$ and because $u_\zeta(\bar{r};\phi,t)$ is small at small Ω. At higher values of Ω, the ζ-circulation plays an increasingly important role in heat advection, but it always transports less heat than the η-circulation. The

contribution of the η-circulation begins to decrease once ΔT_B stops increasing with Ω (see Fig. 2). It is not clear why ΔT_B should stop increasing with Ω at the value it does, except that the maximum ΔT_B permissable must be $\leq \Delta T$. However heat advection by the η and ζ-circulations is unable to account for the total measured heat advection of the fluid at all rotation rates. Because no other processes appear to be present in the fluid, and because eddies may be able to transport significant amounts of heat (as Section 4.5 shows) it seems likely that the remainder of the heat may be transported either by the small scale eddies, or else by the non-geostrophic boundary layers by the sides of the radial barrier.

A consequence of the conclusions relating to the η-circulation [see equation (16)] is that by imposing a temperature difference across the barrier it should be possible to control the η-circulation. A variation on this idea was attempted by Rayer (1995) who replaced the thermally insulating barrier with a thin copper thermally conducting barrier in the hope that this would reduce ΔT_B. However measurements showed that ΔT_B and the fluid heat transfer were largely uneffected, suggesting the formation of signficant boundary layers to the sides of the thermally conducting barrier, which were able to support the temperature drop.

Regarding the eddies, Figure 12(a) shows that no significant heat advection is required of them until $\Omega \sim 3.0$ rad.sec^{-1} at $\Delta T \approx 4$ °C (i.e. when ΔT_B stops increasing with Ω), yet the eddies first appear at $\Omega \gtrsim 1.2$ rad.sec^{-1}. However eddies cannot transport heat effectively until $T'(\bar{r}, z = 0; \phi, t)$ becomes significant. Figure 1(a) shows that even at $\Omega = 1.9$ rad.sec^{-1}, T' is very small because the thermocouple ring data, $T(\bar{r}, z = 0; \phi, t)$ is still closely linear. The values of $\Delta T'$ calculated for $\Delta T \approx 4$ °C plotted in Figure 13 show that $\Delta T'$ increases rapidly between $\Omega \approx 2.5$ rad.sec^{-1} and 3.0 rad.sec^{-1}. This suggests that although the eddies first appear at much lower rotation rates, it is appearance of the temperature perturbations in the thermocouple ring data, $T(\bar{r}, z = 0; \phi, t)$ [see Fig. 1(a)]; that allows them to transport heat effectively. These temperature perturbations start to appear at about the same values of Ω as those at which ΔT_B stops increasing with Ω.

The values of Ω and ΔT for which $u \approx u_\eta$ are those for which all significant heat advection is due to the η-circulation, i.e. $H_{\text{adv}} \approx H_\eta$. In this case $\text{Nu}(\Omega \neq 0) \approx \text{Nu}(\Omega = 0)$ because $u \approx u_0 = u_\eta$. In other words

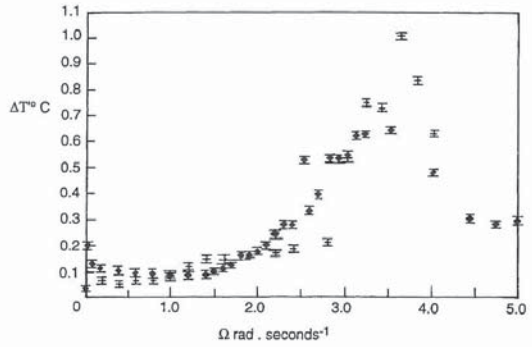

FIGURE 13 Plot of $\Delta T'$ against Ω for the results with the full insulating barrier. For $\Delta T'$ see Section 4.5. The solid diamonds are the $\Delta T \approx 4\,°C$ results and the crosses, the 10 °C results. $\Delta T'$ increases rapidly around 2.5 rad.sec^{-1}.

an azimuthal pressure gradient supported by the radial barrier allows the fluid flow to be the same when $\Omega \neq 0$ as when $\Omega = 0$ [see eqn. (1)], as a consequence the fluid heat transport is independent of Ω and equal to the $\Omega = 0$ value. This is in agreement with Hide's hypothesis [eqn. (1)] which appears to hold for $\Omega \lesssim 3.0$ rad.sec^{-1} at $\Delta T = 4°C$ and for $\Omega \lesssim 4-5$ rad.sec^{-1} at $\Delta T = 10°C$. However at higher values of Ω, even though $u \neq u_0$, Nu remains close to Nu($\Omega = 0$) due to other motions occuring in the fluid.

Acknowledgements

The authors wish to thank R. M. Small and W. N. D. Jackson for their technical support.

References

Bless, S. J., "The effect of a radial barrier on thermally driven motions in a rotating fluid annulus," B.Sc. thesis, Massachusets Institute of Technology, U.S.A. (1965).
Bowden, M., "An experimental investigation of heat transfer in rotating fluids," Ph.D. thesis, University of Durham (now the University of Newcastle-upon-Tyne) (1961).

Bowden, M. and Eden, H. F., "Effect of a radial barrier on the convective flow in a rotating fluid annulus," *J. Geophys. Res.* **73**, 6887–6896 (1968).
Fowlis, W. W. and Hide, R., "Thermal convection in a rotating annulus of liquid: effect of viscosity on the transition between axisymmetric and non-axisymmetric flow regimes," *J. Atmos. Sci.* **22**, 541–558 (1965).
Hide, R., "Some experiments on thermal convection in a rotating fluid," in: *Procedings of the first symposium on the use of models in geophysical fluid dynamics*, (Ed. R. R. Long, pp. 101–116), Washington, D. C.: U.S. Government Printing Office (see also *Quart. J. Roy. Meteorol. Soc.* **79**, 161) (1953).
Hide, R., "An experimental study of thermal convection in a rotating liquid," *Phil. Trans. R. Soc. Lond.* **A250**, 442–478 (1958).
Hide, R., "On source-sink flows in a rotating fluid," *J. Fluid. Mech.* **32**, 737–764 (1968).
Hide, R., "Experiments with rotating fluids," *Quart. J. Roy. Met. Soc.* **103**, 435, 1–28 (1977).
Hide, R., "On the effects of rotation on fluid motions in containers of various shapes and topological characteristics," *Dyn. Atmos. Oceans* (in press) (1997).
Hide, R. and Mason, P. J., "Baroclinic waves in a rotating fluid subject to internal heating," *Phil. Trans. R. Soc. Lond.* **A268**, 201–232 (1970).
Hide, R. and Mason, P. J., "Sloping convection in a rotating fluid," *Adv. in Phys.* **24**(1), 47–100 (1975).
Hide, R., Lewis, S. R. and Read, P. L., "Sloping convection: A paradigm for large-scale waves and eddies in planetary atmospheres?" *Chaos.* **4**, 135–162 (1994).
Hide, R., Mason, P. J. and Plumb, R. A., "Thermal convection in a rotating fluid subject to a horizontal temperature gradient: spatial and temporal characteristics of fully developed baroclinic waves," *J. Atmos. Sci.* **34**(6), 930–950 (1977).
Hignett, P., White, A. A., Carter, R. D., Jackson, W. N. D. and Small, R. M., "A comparison of laboratory measurements and numerical simulations of baroclinic wave flows in a rotating cylindrical annulus," *Quart. J. Roy. Met. Soc.* **111**, 131–154 (1985).
Jonas, P. R. and Kent, P. M., "Two-dimensional velocity measurements by automatic analysis of trace particle motion," *J. Phys. E: Sci. Instrum.* **12**, 604–609 (1979).
Kreith, F., "Convective heat transfer in a rotating system," *Advances in Heat Transfer* **5**, 129–251 (1968).
Prandtl, L., Essentials of fluid dynamics. New York, Hafner publishing Company (1952).
Rayer, Q. G., "An experimental investigation of heat transfer by large-scale motions in rotating fluids," D.Phil. thesis, Oxford University, U.K., 250 pages (1992).
Rayer, Q. G., "A numerical investigation of the flow in a fully blocked differentially heated rotating fluid annulus," *J. Modern Physics C–Physics & Computers* **5**(2), 203–206 (1994).
Rayer, Q. G., "Thermal convection in a rotating fluid annulus blocked by a conducting barrier," IMechE Transactions, 4th U.K. National Conference on Heat Transfer, ISSN 1356–1448, ISBN 0-85298-950-4, pp. 177–181 (1995).
Tritton, D. J., Physical fluid dynamics O.U.P., ISBN 0-19-854493-6, 519 pages (1988).

APPENDIX: SOME THEORETICAL CONSIDERATIONS BY R. HIDE

The experiments described above extend other work along lines indicated by theoretical considerations of effects of Coriolis forces due

to general rotation on buoyancy-driven flows in cylindrical containers of various shapes (cf. Hide, 1968). In general Coriolis forces affect not only the (Eulerian) field of relative flow $\mathbf{u}(\mathbf{r}, t)$ but also fields of pressure $p(\mathbf{r}, t)$, density $\rho(\mathbf{r}, t)$, etc. (where t denotes time and $\mathbf{r}$ is the position of a general point R in a reference frame attached to the apparatus, which rotates with steady angular velocity Ω relative to an inertial frame). But there are certain special cases, characterized by the topology of the boundaries, in which rotation affects $p(\mathbf{r}, t)$ and $\rho(\mathbf{r}, t)$ in such a way as to leave $\mathbf{u}(\mathbf{r}, t)$ unchanged or when the changes are small. For further details of the following discussion see Hide (1997).

Consider an incompressible fluid of uniform chemical composition in which the density

$$\rho(\mathbf{r}, t) = \bar{\rho}[1 + \theta(\mathbf{r}, t)], \tag{A.1}$$

where $\bar{\rho}$ is the mean density, depends only on temperature $T(\mathbf{r}, t)$; thus

$$\theta(\mathbf{r}, t) = -\alpha[T(\mathbf{r}, t) - \bar{T}], \tag{A.2}$$

if α is the thermal coefficient of cubical expansion and $\bar{T}$ the mean temperature. For such a fluid the respective equations of mass conservation, momentum and heat transfer are the following:

$$\nabla \cdot \mathbf{u} = 0, \tag{A.3}$$

$$\frac{D\mathbf{u}}{Dt} + 2\boldsymbol{\Omega} \times \mathbf{u} = -\nabla(P + V) + \theta \nabla V + \nu \nabla^2 \mathbf{u}, \tag{A.4}$$

where $D/Dt \equiv \partial/\partial t + \mathbf{u} \cdot \nabla$, $P(\mathbf{r}, t) \equiv p(\mathbf{r}, t)/\bar{\rho}$, ν is the coefficient of kinematic viscosity and $-\nabla V$ the acceleration due to gravity plus centrifugal effects and

$$\frac{D\theta}{Dt} = \kappa \nabla^2 \theta - q, \tag{A.5}$$

where κ is the coefficient of thermal diffusivity ($\kappa \bar{\rho} c$ being the thermal conductivity if c is the specific heat) and $q \bar{\rho} c \alpha$ is the diabatic heating rate due to any internal thermal sources that might be present within the fluid. When V and q are specified *ab initio*, (A.1) to (A.5) suffice with the appropriate thermal and mechanical boundary conditions to determine the six independent variables P, θ, T and the three

components of $\mathbf{u}$, all in general functions of $\mathbf{r}$ and t. There may of course be multiple solutions of these essentially nonlinear equations, for which there are in general no uniqueness theorems.

Equation (A.4) expresses the instantaneous balance of forces acting on the element of fluid of unit mass at the general point R. The corresponding balance of torques expressed by

$$\frac{D\boldsymbol{\xi}}{Dt} - ((\boldsymbol{\xi} + 2\boldsymbol{\Omega}) \cdot \nabla)\mathbf{u} - \nu \nabla^2 \boldsymbol{\xi} = \nabla V \times \nabla \theta \tag{A.6}$$

(where $\boldsymbol{\xi} \equiv \nabla \times \mathbf{u}$), obtained by taking the curl of (A.4). A "baroclinic" fluid is defined as having density variations on level surfaces, in which the right-hand side of (A.6) is not zero and hydrostatic equilibrium (i.e., $\mathbf{u} = \mathbf{0}$ everywhere) is impossible. When, by contrast, $\nabla V \times \nabla \theta = \mathbf{0}$ everywhere, the fluid is said to be "barotropic"; then there are no torques exerted by buoyancy forces and (in the absence of relative motion between different parts of the boundary surfaces) hydrostatic equilibrium becomes possible.

Equation (A.6) leads directly to the useful expression

$$\frac{DQ}{Dt} = (2\boldsymbol{\Omega} + \boldsymbol{\xi}) \cdot \nabla \frac{D\Lambda}{Dt} + \nabla \Lambda \cdot \nabla V \times \nabla \theta + \nu \nabla \cdot \nabla^2 \boldsymbol{\xi}, \tag{A.7}$$

where $\Lambda = \Lambda(\mathbf{r}, t)$ is any continuous and differentiable scalar quantity and the pseudo-scalar

$$Q \equiv (2\boldsymbol{\Omega} + \boldsymbol{\xi}) \cdot \nabla \Lambda \tag{A.8}$$

is the so-called "Ertel potential vorticity". In the important special case when $\Lambda = \theta$ and $\nu = \kappa = q = 0$, the quantity $Q' \equiv (2\boldsymbol{\Omega} + \boldsymbol{\xi}) \cdot \nabla \theta$ is conserved on a moving fluid element, for then, by (A.5) and (A.7) $DQ'/Dt = 0$.

Let ($\mathbf{u}_0$, P_0, θ_0, etc.) be solutions of (A.3) – (A.5) when $\boldsymbol{\Omega} = \mathbf{0}$ and ($\mathbf{u}_0 + \mathbf{u}_1$, $P_0 + P_1$, $\theta_0 + \theta_1$, etc.) when $\boldsymbol{\Omega} \neq \mathbf{0}$. Direct substitution shows that $\mathbf{u}_1 = \mathbf{0}$ when $\boldsymbol{\Omega} \neq \mathbf{0}$ (but gravity $\mathbf{g} \equiv -\nabla V_0$ is so strong that centripetal effects make a negligible contribution to ∇V) if the following conditions are satisfied eveywhere:

$$2(\boldsymbol{\Omega} \cdot \nabla)\mathbf{u}_0 = \mathbf{g} \times \nabla \theta_1 \tag{A.9}$$

and

$$2\boldsymbol{\Omega} \times \mathbf{u}_0 = -\nabla P_1 + \mathbf{g}\theta_1. \tag{A.10}$$

Suppose now that $\boldsymbol{\Omega}$ and $\mathbf{g}$ are antiparallel vectors $\Omega\hat{\mathbf{k}}$ and $-g\hat{\mathbf{k}}$ respectively, where $\hat{\mathbf{k}}$ is a unit vector in the direction of increasing z (say). When integrated around any continuous closed curve C in a plane where z is constant that lies everywhere within the fluid, Equation (A.9) gives

$$2\Omega \frac{\partial}{\partial z} \oint_C \mathbf{u}_0 \cdot d\mathbf{c} = -g\hat{\mathbf{k}} \cdot \oint_C \nabla\theta_1 \times d\mathbf{c}. \tag{A.11}$$

Correspondingly, (A.10) gives

$$2\Omega\hat{\mathbf{k}} \cdot \oint_C \mathbf{u}_0 \times d\mathbf{c} = -V_0 \oint_C \nabla\theta_1 \cdot d\mathbf{c} = 0, \tag{A.12}$$

since θ_1 must be single valued (cf. Hide, 1958; Hide and Mason, 1970; Hide *et al.*, 1994).

Figure A1 illustrates the meridional circulation produced by buoyancy forces in a fluid annulus when the temperature T_b of the outer wall exceeds that of the inner wall T_a. As in the analogous source-sink flow in a barotropic fluid (see Hide, 1968, Fig. 1a) it is possible in this case to find circuits C for which (A.12) is not satisfied, such as circles concentric with the axis of the system, implying that $\mathbf{u}_0$ cannot be a solution when $\Omega \neq 0$. In this case Coriolis forces inhibit meridional overturning, thereby reducing advective heat transfer, and they induce a flow $\mathbf{u}_\phi$ in the azimuthal (ϕ) direction. In average magnitude, this flow increases linearly with Ω when Ω is small and decreases as Ω^{-1} when Ω is large, implying that a maximum value is attained at some critical value of Ω. Coriolis forces also promote non-axisymmetric "baroclinic instability" at sufficiently high values of Ω (in excess of the abovementioned critical value). This leads to "sloping convection" (Hide, 1958; Hide and Mason, 1975) which enhances advective heat transfer to a level in excess of that associated with axisymmetric flow, but still less than in the case when $\Omega = 0$.

Now consider a case when the meridional cross-section of the annular apparatus is blocked by a thin impermeable radial barrier [see

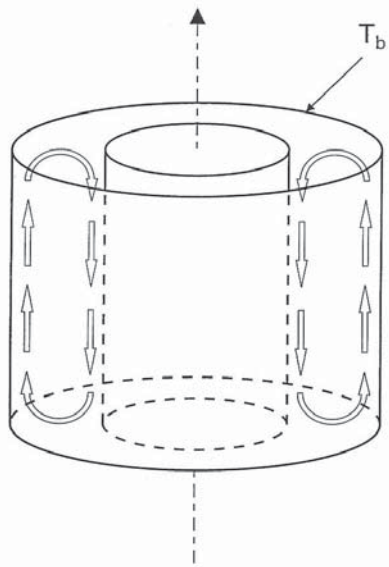

FIGURE A1 Illustrating the meridional cirulation induced in a non-rotating annulus subject to an impressed horizontal temperature gradient (in the case when the outer cylinder is hotter than the inner cylinder, i.e. $T_b > T_a$).

Fig. 8, the analogous source-sink arrangement in a barotropic fluid being illustrated by Fig. 2(a) of Hide (1968)]. The cross-section of the apparatus is now topologically simply-connected, rather than doubly-connected as when the barrier is absent, and it is possible to find circuits C for which (A.11) is satisfied. This implies that $\mathbf{u}_0$ might be a solution when $\Omega \neq 0$, and that if such a solution exists it would be accompanied by additional fields of pressure P_1 and density θ_1 with gradients in the ϕ direction only satisfying (A.9) and (A.10). Such gradients could now be supported owing to the presence of the barrier, across which jumps of P_1 and θ_1 would occur.

This hypothetical theoretical case is not expected to occur in practice, except perhaps at fairly low values of Ω, but its properties are useful as a guide to systematic experimental investigations, such as those presented in the main part of this paper. Theoretical considerations along the lines presented above were first used in the interpretation of observed flow patterns and heat transfer determinations in experiments with the annular system without a radial barrier (Hide, 1958). They also provided the qualitative basis of my hypothesis that the insertion of a radial barrier would increase advective heat transfer, possibly to the level corresponding to $\Omega = 0$, in favour of which there is now ample evidence (Bowden, 1961; Bowden and Eden, 1968; Rayer, 1992 and the main body of this paper) from experiments carried out in my laboratory. The range of Ω over which heat transfer is found to be the same as for $\Omega = 0$, is so large that it cannot be accounted for without invoking, in addition to a circulation in meridional planes, a motion $\mathbf{u}_h$ with horizontal components, seen in the experiments, which must make an increasing contribution to the heat transfer H as Ω increases (see Fig. 8).

It is customary in fluid dynamics to measure total heat transfer H in terms of the dimensionless Nusselt number, Nu defined as the total heat transfer H divided by that which would occur by conduction (and radiation) alone if the fluid were replaced by a solid with the same thermal properties (see e.g. Prandtl, 1952; Hide, 1958). By general considerations based directly on the governing equations and boundary conditions, or on dimensionless analysis above, suffice to show that

$$\mathrm{Nu} = \mathrm{Nu}(\Theta, \tau, \Pi, A), \tag{A.13}$$

in which

$$\Theta \equiv \frac{g\alpha|T_b - T_a|d}{\Omega^2(b-a)^2} \tag{A.14}$$

(Hide, 1958);

$$\tau \equiv \frac{4\Omega^2(b-a)^5}{\nu^2 d} \tag{A.15}$$

(Fowlis and Hide, 1965);

$$\Pi \equiv \frac{\nu}{\kappa}, \tag{A.16}$$

the Prandtl number; and the parameter

$$A = A[(b-a)/(b+a), (b-a)/d] \tag{A.17}$$

depends only on geometrical quantities b, a, and d.

The significance of Θ and τ emerged from wide-ranging experiments on thermal convection in a rotating fluid annulus as the independent parameters that *inter alia* (together with Π and A to a lesser extent) largely determine which of a rich variety of axisymmetric and non-axisymmetric flow regimes will occur. The more familiar Grashof number

$$G \equiv \frac{g\alpha|T_b - T_a|(b-a)^3}{\nu^2} \tag{A.18}$$

equal to Π times the equally-familiar Rayleigh number, is not to be regarded as an independent parameter here, for $G = \Theta\tau$, but it is significant that $\mathrm{Nu} = 0.4G^{1/4}$ (see Prandtl, 1952) when $\Omega = 0$.

Another theoretically important quantity which, like Nu, can be measured in a fairly straightforward way and whose dependence on the parameters Θ, τ, Π, and A deserves further study, is the meridionally-averaged jump in the temperature across the radial barrier, here denoted by ΔT_ϕ and conveniently expressed in terms of the dimensionless parameter

$$\eta \equiv \frac{|\Delta T_\phi|}{|T_b - T_a|}. \tag{A.19}$$

As with the Nusselt number Nu, general considerations suffice to show that

$$\eta = \eta(\Theta, \Pi, \tau, A). \tag{A.20}$$

Equivalent to (and more convenient than) (A.20) is the relationship

$$\eta = \eta(\Omega/\Omega^*), \tag{A.21}$$

where Ω^* is some "scale angular speed of rotation", to be determined by theory or experiment.

It can be argued that the dependence is linear when $\Omega/\Omega^* \ll 1$ and that when $\Omega/\Omega^* \gg 1$, owing to the requirement that isotherms be conserved, η tends asymptotically to a constant value less than unity. If the variation of η with Ω/Ω^* is monotonic then it must have the general form illustrated in Figure A2.

As expression for Ω^* can be deduced by applying (A.9) in the case when $\Omega \ll \Omega^*$. Thus, if $2\Omega\Delta U_0/d$ is a measure of the average magnitude the radial component of $(2\boldsymbol{\Omega}\cdot\nabla)\mathbf{u}_0$, then

$$\eta = \left\{\Omega \frac{2\pi(b+a)\Delta U_0}{Mg\alpha|T_b - T_a|d}\right\} \tag{A.22}$$

(when $\Omega < \Omega^*$), so that

$$\Omega^* = \frac{Mg\alpha|T_b - T_a|d}{2\pi(b+a)\Delta U_0} \tag{A.23}$$

which could, in principle, be related to Π, A and G. Here we have included the extra parameter M, the number of equally-spaced thin barriers in cases when $M \neq 1$.

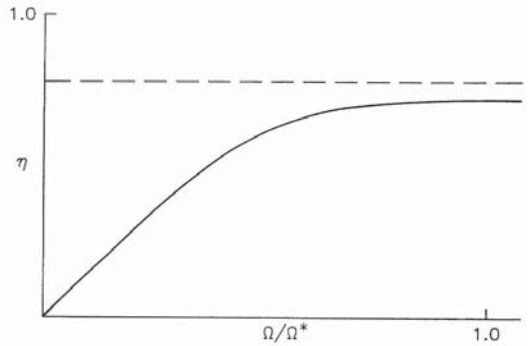

FIGURE A2 Schematic dependence of η on Ω/Ω^* (see text).

It is not yet possible to predict the exact form of $\eta(\Omega/\Omega)$ over the whole range, but the following considerations of the relative potential vorticity

$$\sigma \equiv \boldsymbol{\xi}\cdot\nabla\theta \tag{A.24}$$

are probably relevant. In the terminology of (A.9), (A.10) etc., we write $\sigma = \sigma_0 + \sigma_1$, where

$$\sigma_0 = \boldsymbol{\xi}_0\cdot\nabla\theta_0 \tag{A.25}$$

and

$$\sigma_1 = \boldsymbol{\xi}_0\cdot\nabla\theta_1 + \boldsymbol{\xi}_1\cdot\nabla_0 + \boldsymbol{\xi}_1\cdot\nabla\theta_1. \tag{A.26}$$

In the absence of rotation (i.e., when $\Omega = 0$) not only are $\sigma_1 = \boldsymbol{\xi}_1 = \nabla\theta_1 = 0$ by definition, but so is σ_0 equal to zero because $\mathbf{u}_0$ lies everywhere in meridian planes and θ_0 depends on meridional coordinates, but not on ϕ, the azimuthal coordinate. The extent to which the vorticity vector $\boldsymbol{\xi}$ remains perpendicular to $\nabla\theta$ when $\Omega \neq 0$ should be investigated, for it is clear by inspection of Figure 8 that the meridional and horizontal circulations make contributions of opposite sign to σ. Equilibration might be characterized by the cancelling of these respective contributions, a hypothesis which could guide to future laboratory and numerical investigations, in which the ratio Γ (say) of the magnitudes of these two contributions to σ could easily be determined.

Important results have already been obtained from systematic laboratory studies of annular systems with and without radial barriers, and also with related triply-connected non-annular systems (unpublished), but much more remains to be done if the full potential of such work is to be realized. Obvious difficulties are presented by the number of independent parameters to be covered. Some mitigation of these difficulties is offered by the material presented in this Appendix.